

# From nonlinear scaling fields to critical amplitudes

Y. Meurice and S. Niermann

*Department of Physics and Astronomy, The University of Iowa, Iowa City, Iowa 52242,  
USA*

## Abstract

We propose to combine the nonlinear scaling fields associated with the high-temperature (HT) fixed point, with those associated with the unstable fixed point, in order to calculate the susceptibility and other thermodynamic quantities. The general strategy relies on simple linear relations between the HT scaling fields and the thermodynamic quantities, and the estimation of RG invariants formed out of the two sets of scaling fields. This estimation requires convergent expansions in overlapping domains. If, in addition, the initial values of the scaling fields associated with the unstable fixed point can be calculated from the temperature and the parameters appearing in the microscopic Hamiltonian, one can estimate the critical amplitudes. This strategy has been developed using Dyson's hierarchical model where all the steps can be approximately implemented with good accuracy. We show numerically that for this model (and a simplified version of it), the required overlap apparently occurs, allowing an accurate determination of the critical amplitudes.

Keywords: Renormalization group, scaling fields, high-temperature expansion, hierarchical model, normal forms, critical amplitudes, crossover.

# I. INTRODUCTION, MOTIVATIONS AND MAIN RESULTS

It is well-known that the magnetic susceptibility of a spin model near its critical temperature can be parametrized as

$$\chi = (\beta_c - \beta)^{-\gamma} (A_0 + A_1(\beta_c - \beta)^\Delta + \dots) . \quad (1.1)$$

In this expression, the exponents  $\gamma$  and  $\Delta$  are universal and can be obtained from the calculation of the eigenvalues of the linearized renormalization group (RG) transformation. On the other hand, the critical amplitudes  $A_0, A_1, \dots$  are functions of the microscopic details of the theory. One can find universal relations [1] among these amplitudes and the ones associated with other thermodynamic quantities, however these relations do not fix completely the amplitudes. In the end, if we want a quantitative estimate of a particular amplitude, we need to perform a calculation which requires a knowledge of many details of the RG flows. Such a calculation is in general a difficult, nonlinear, multivariable problem. In this article we propose a general strategy based on the construction of nonlinear scaling fields associated with *several* fixed points, to calculate the critical amplitudes, and we demonstrate its feasibility in the case of Dyson's hierarchical model.

A common strategy in problems involving nonlinear flows near a singular point, is to construct a new system of coordinates for which the governing equations become linear. It seems intuitively clear that if the original problem is sufficiently nontrivial, normal form methods can only work in some limited way, locally, because the flows of the nonlinear problem have global properties which do not match those of the linear flows. A well-known argument for the inadequacy of such procedure (which extends beyond the special case of an expansion near a singular point) was provided by Poincaré [2] in the context of perturbed integrable Hamiltonians. He discovered that even though it is possible to write a formal perturbative series for the action-angle variables, some coefficients have “small denominators”, and generically, the series are ill-defined. However, under some restrictions (formulated according to some appropriate version of the K. A. M. theorem [3]), perturbation theory can still provide interesting information.

Almost thirty years ago, Wegner [4], introduced quantities that transformed multiplicatively under a RG transformation. He called them “scaling fields” and we will use his terminology in the following. Sometimes, one also uses the terminology “nonlinear scaling field” to distinguish them from the linear ones (see section II for details). In the following, “scaling fields” mean the nonlinear ones and we will use the terminology “linear scaling fields” when necessary. These fields play a central role in the presentation of the basic ideas of the RG. They appear in almost any review on the subject (see for instance Ref. [5]). As in the case of Hamiltonian dynamics, there exists a formal series expansion for the scaling variables (see Eq. (4.9) in Ref. [4]). It is commonly assumed that the functions defined with this procedure are analytic, at least within a certain neighborhood of the fixed point. However, for most non-trivial models, it is very difficult to prove this assumption. In particular, it is difficult to address the question of small denominators because it requires an accurate calculation of the eigenvalues of the linearized RG transformation.

If the small denominator problem can be controlled and if some *local* expansion is well-defined, there remain several important *global* issues. What is the domain of convergence of this expansion? How does the accuracy of an expansion with a finite number of terms evolve

when we move away from the fixed point? Can different expansions have overlapping domain of convergence? These important *global* issues are rarely discussed because of practical limitations: in crossover regions, we need large order expansions in many variables. Unfortunately, this problem has to be faced if we want to calculate all the critical amplitudes. In this article, we propose a general strategy to calculate directly the critical amplitudes. This strategy has been developed using Dyson's hierarchical model, where large order expansions in many variables are practically feasible. All the numerical calculations presented hereafter were done with this model (or a simplified version of it).

The general point of view that we want to advocate here is that one should combine different sets of scaling fields. Even though the scaling fields are almost always constructed in the vicinity of Wilson's fixed point, they can in principle be constructed near any other fixed point. If one can find some overlap among the domains of convergence of these expansions it is possible to reconstruct the flows, given their initial values. In other words, we would like to develop a new analytical approach to complement the existing methods used to deal with the crossover between fixed points, namely, the Monte Carlo method [6–8], a combination of field-theoretical methods and mean field calculations [9,10] or the study of the entropy associated with the RG flows [11].

In the following, we concentrate on the study of the RG flows in the symmetric phase of spin models having a nontrivial unstable fixed point. Our goal is to calculate the critical amplitudes by constructing the scaling fields near the three relevant fixed points: the Gaussian fixed point (if relevant), the unstable fixed point (sometimes called the IR fixed point or Wilson's fixed point), and the high-temperature (HT) fixed point. The idea is represented schematically in Fig. 1.

We propose to follow three specific steps to achieve this goal. These steps correspond to a construction in backward order, starting with the flows near the HT fixed point and ending with the initial conditions. First, we express the thermodynamic quantities in terms of the scaling fields of the HT fixed point. Second, we use the scaling fields of the unstable IR fixed point, to write the thermodynamic quantities as a main singularity times a RG invariant quantity constructed out the two scaling fields. Third, we calculate the initial values of the scaling fields associated with the unstable fixed point in terms of the basic parameters appearing the microscopic Hamiltonian. These three steps are explained in more detail in Section II. This section is essential to understand the general ideas and the notations used later. It should be noted that the first two steps are independent of the initial conditions and are in some sense universal. On the other hand, the third step provides the initial data as a function of the basic parameters such as the temperature or the “bare parameters” of Landau-Ginzburg models. Consequently, the method used to implement the third step depends on the initial measure considered. For instance, if we start with an initial measure near the Gaussian fixed point, perturbative field theoretical methods (Feynman diagrams) will be used.

Each of these three steps can in principle be implemented for spin models with nearest neighbor interactions in three dimensions, by using available expansions to describe the flows in each region. However, in order to discuss the behavior of the expansions in the crossover region, we need large order expansions. Despite the existence of increasingly sophisticated methods used for various expansions in nearest neighbor models (see e.g., Ref. [12]), it is still a major time investment to perform these expansions. In order to

test the feasibility of the procedure, we have considered approximations for which large order expansions (see e.g., Refs. [13,14]) can be reached more easily. Namely, we have used hierarchical approximations where only the local part of the measure is renormalized under a RG transformation. Well-known examples are the “approximate recursion formula” [15] or Dyson’s hierarchical model (HM) [16,17]. Despite this approximation, the nonlinear aspects of the problem are still nontrivial. To fix the ideas, the calculations that we have performed required the determination of several thousands of coefficients in various expansions.

The relevant facts about the HM and its RG transformation are reviewed in Section III. Before embarking in a multivariable calculation, we have first considered a simplified version involving only one variable [18] where the small denominator problem is obviously absent. This model discussed in Section IV, is simply a quadratic map with two fixed points, one stable and one unstable. Series expansions for the scaling fields of this simplified model, and their inverse, can easily be constructed. Treating these numerical series with well-known estimators [19], we obtain radii of convergence and exponents in very good agreement with what we can infer by using general arguments. These numerical results will be used as references when a similar analysis is conducted later for the HM. The most important result of Section IV is illustrated Fig. 5 which shows that the expansions of the scaling fields scale accurately in overlapping regions.

The rest of the article is devoted to the HM with one spin component per site (as in the Ising model). For this model, the existence of a non-trivial unstable fixed point has been proven rigorously [20,21]. Significant results have been obtained regarding the *local* existence of scaling fields for the RG map near the unstable fixed point by Collet and Eckmann [21] and Koch and Wittwer [22]. In addition, Ref. [22] contains a mathematical justification of the polynomial approximations that we have used to perform large order HT expansions [13,14] or direct numerical calculations [23,24]. In the following, the parameter playing the role of the dimensionality (see Section III) will be tuned in such way that a Gaussian massless field scales exactly as in three dimensions. In other words, we will work at an intermediate value between the upper and lower critical dimensions and the  $\epsilon$ -expansion is not obviously useful. For this particular choice of the dimensionality parameter, the numerical value of the unstable fixed point is known with great precision in a specific system of coordinates [25] and the question of small denominators studied in Ref. [26].

Using these results we first provide an explicit construction of the two sets of scaling fields and show that the first two steps can be implemented. We found simple linear relations between the derivatives of the free energy and the HT scaling fields. The RG invariants discussed above can be calculated accurately (see Fig. 14) because the scaling fields associated with the two fixed points scale accurately in overlapping regions as shown in Fig. 13. The third step was performed in the case of an initial Ising measure where the temperature is the only free parameter. Putting everything together, we can calculate the leading and subleading amplitude of the susceptibility and have very good agreement with previous numerical calculations [24]. This demonstrates the feasibility of the proposed strategy. In the conclusions, we discuss our plans to extend this method for perturbative initial conditions and for nearest neighbor models.

A few words of caution. We want to make clear that the main result presented in this article is a calculation of the leading and subleading critical amplitudes of the magnetic susceptibility of the hierarchical model. This calculation shows that the strategy discussed

in the coming section II can be implemented successfully for this particular model. The fact that part of the introduction and Section II are written for a general spin model should not be interpreted as the statement that it is straightforward to implement the strategy for other models than the hierarchical model. The reader whose main interest is the hierarchical model may read section II as a general description of what is done in the rest of the paper. On the other hand, the reader interested in using the general strategy for other models, should be aware that we do not provide a general procedure for constructing the unstable fixed point and its scaling fields. In addition, the fact that we found overlapping domain of convergence in the particular computation presented here is an encouraging result but it does not guarantee that a similar overlap will be found for other models.

## II. THREE STEPS TOWARDS THE CALCULATION OF THE CRITICAL AMPLITUDES

In this section, we consider a scalar model on a  $D$ -dimensional lattice with a lattice spacing  $a_0$ . We assume that  $\beta < \beta_c$  and that the free energy density  $f$  is finite in the thermodynamic limit. We discuss the estimation of the critical amplitudes in the HT phase for  $\chi^{(l)}$ , the  $l$ -th derivative of  $-f$  with respect to an external magnetic field. For definiteness, we generalize the parametrization of Eq. (1.1) to

$$\chi^{(l)} = (\beta_c - \beta)^{-\gamma^{(l)}} (A_0^{(l)} + A_1^{(l)}(\beta_c - \beta)^{\Delta^{(l)}} + \dots) . \quad (2.1)$$

We assume the existence of a discrete RG transformation  $\mathbf{R}$ , which can be performed in the following way. We first integrate the fields in blocks of side  $ba_0$  while keeping the sum of the fields in the block constant. We then rescale the sums of the fields by a factor  $b^{(-2-D+\eta)/2}$ . For the HM,  $b = 2^{1/D}$  and  $\eta = 0$ . We assume that this RG transformation has one non-trivial unstable fixed point and an attractive HT fixed point. We first introduce general notations for the scaling fields and then discuss the three steps.

### A. Construction of the scaling fields

A preliminary requisite is the construction of the two sets of scaling fields. We construct the scaling fields near the unstable fixed point, denoted  $\mathbf{y}(\mathbf{d})$ , in terms of the coordinates  $\mathbf{d}$  in the directions of the eigenvectors of the linearized RG map at that fixed point. The boldface notations mean that the quantity is a vector. In the following we will consider finite dimensional approximations for such vectors. For small values of  $\mathbf{d}$ , we have  $\mathbf{y}(\mathbf{d}) \simeq \mathbf{d}$ . One could call the  $\mathbf{d}$ , the “linear scaling fields” or the “real fields” [4] if they have a simple physical interpretation. If we denote the RG transformation in the  $\mathbf{d}$  coordinates as  $\mathbf{R}(\mathbf{d})$ , and  $\lambda_j$  as the eigenvalue in the  $j$ -th direction, we have by definition of the scaling fields

$$y_j(\mathbf{R}(\mathbf{d})) = \lambda_j y_j(\mathbf{d}) . \quad (2.2)$$

In the following, we assume that the spectrum is real, positive, non-degenerate and that only  $\lambda_1 > 1$ .

Similarly, the HT scaling fields denoted  $\tilde{\mathbf{y}}(\mathbf{h})$ , can be constructed as expansions in the coordinates  $\mathbf{h}$  in the directions of the eigenvectors of the linearized RG map at the HT fixed point. With notation analog to Eq. (2.2), we have

$$\tilde{y}_j(\mathbf{R}(\mathbf{h})) = \tilde{\lambda}_j \tilde{y}_j(\mathbf{h}). \quad (2.3)$$

The  $\mathbf{d}$ 's can be expressed in terms of the  $\mathbf{h}$ 's by a shift followed by a linear transformation. In the following  $y_{n,l}$  or  $y_l(\mathbf{d}_n)$  will denote the value of the  $l$ -th scaling field after  $n$  iterations, and similar notations will be used for the HT variables.

### B. step 1

The first step consists in expressing the  $\chi^{(l)}$  in terms of the scaling fields of the HT fixed point  $\tilde{\mathbf{y}}$ . In the vicinity of the HT fixed point, the effective lattice spacing becomes larger than the physical correlation lengths. This fixed point is attractive and as the number of iterations  $n$  becomes large, one can treat the blocks as almost isolated systems with a large volume  $b^{nD}$ . In the following we call  $\chi_n^{(l)}$  the average value of the  $l$ -th power of the total spin in this volume minus its disconnected parts, divided by the volume. Assuming that  $\lim_{n \rightarrow \infty} \chi_n^{(l)} = \chi^{(l)}$  is finite for  $\beta < \beta_c$ , we conclude that the subtracted average value of the  $l$ -th power of the *rescaled* sum of all the spins scales like  $b^{-((2+D-\eta)(l/2)-D)n}$  for  $n$  large and should be expressible as products of the  $\tilde{\mathbf{y}}$  with product of eigenvalues  $b^{-((2+D-\eta)(l/2)-D)}$ . Indeed, in explicit calculations for the HM model, we found that simple linear relations hold, namely, when  $n$  becomes large

$$\chi_n^{(2q)} \propto \tilde{y}_q(\mathbf{h}_n) (\tilde{\lambda}_q)^{-n}, \quad (2.4)$$

and consequently,

$$\chi^{(2q)} = K^{(q)} \tilde{y}_q(\mathbf{h}_{in}), \quad (2.5)$$

with  $\mathbf{h}_{in}$  denoting the initial values and  $K^{(q)}$  a constant depending on the choice the scales of the coordinates  $\mathbf{h}$  and easily calculable. This is discussed explicitly in subsection VC for the HM. For the simplicity of the exposition, we will assume that this is also true for other models. Nevertheless it is straightforward to generalize the construction for the case of products of HT scaling fields.

### C. Step 2

The expansion of  $\tilde{y}_q(\mathbf{h}_{in})$  is expected to converge for  $\mathbf{h}_{in}$  small enough, however it might not be very useful or even meaningful near the unstable fixed point or the Gaussian fixed point. If  $\gamma^{(2q)}$  denotes the leading critical exponent for  $\chi^{(2q)}$ , it follows from arguments based on the linear RG transformation that  $\gamma^{(2q)} = -\ln \tilde{\lambda}_q / \ln \lambda_1$ . Consequently,  $y_1^{\gamma^{(2q)}} \tilde{y}_q$  is RG-invariant. We can then factor out the susceptibility into a singular part and a RG invariant part:

$$\chi^{(2q)} = K^{(q)} [y_1(\mathbf{d}(\mathbf{h}_{in}))]^{-\gamma^{(2q)}} \left[ [y_1(\mathbf{d}(\mathbf{h}_{in}))]^{\gamma^{(2q)}} \tilde{y}_q(\mathbf{h}_{in}) \right]. \quad (2.6)$$

The factor in large brackets is RG-invariant and does not need necessarily to be evaluated for initial values of  $\mathbf{h}$ . We can use the  $n$ -th iterate of these values  $\mathbf{h}_n = \mathbf{R}^n(\mathbf{h}_{in})$  for any  $n$  and get the same answer. In particular, we can choose  $n$  is such a way that the flow is “in between” the two fixed points considered here, in a crossover region where the two expansions have a chance to be valid. One of the main results presented in this article are numerical evidences that this procedure actually works. In other words, that there exists an overlap between the domains where approximate expansions of the scaling fields scale as they should.

The scaling properties of expansions are related to convergence issues which need to be discussed in the complexification of the construction. If an eigenvalue appearing in the defining equation for the scaling fields Eqs. (2.2) and (2.3), is such that  $|\lambda_l| \neq 1$ , it is clear that the only values that can be taken by  $|y_l|$  at a fixed point are 0 and  $\infty$ . Consequently, a detailed analysis of the fixed points for the complexification of the RG transformation can put restrictions on the domain of convergence of the scaling fields. Later, the inverse functions  $\mathbf{d}(\mathbf{y})$  or  $\mathbf{h}(\tilde{\mathbf{y}})$  will also be used. Their radius of convergence can be restricted by the study of the extrema of the original function. In the case of the one dimensional model of Section IV, such a study can be conducted easily and confirms the results of the numerical analysis.

Near criticality, for the values of  $n$  in the crossover discussed above, the values of the scaling fields associated with the irrelevant directions are usually very small (unless very large initial values have been chosen) and can be treated perturbatively. In first approximation, we can consistently set the initial values of the irrelevant scaling fields to zero since they are multiplicatively renormalized. In this approximation, we describe the flow along the unstable manifold. A local calculation involving a scaling field corresponding to the the relevant direction is provided in Ref. [22] following a procedure developed in Ref. [27] to prove Feigenbaum conjectures.

It should also be noted that since the RG considered here is discrete (it is constructed by iterating  $\mathbf{R}$  an integer number of times), RG-invariant does not mean independent of  $\mathbf{h}_{in}$ . There is room for log-periodic corrections, which have been first noticed by Wilson [15], discussed in general in Ref. [28] and observed in the HT expansion of the HM in Refs. [13,14]. These corrections are studied for the simplified model in Section IV. In our numerical study of the HM of Section III, these corrections are too small to be resolved and will be ignored.

### D. Step 3

In the previous step, we traded a difficult problem (the estimation of the initial values of  $\tilde{\mathbf{y}}$ ) for two simpler problems: the estimation of the RG invariant and the estimation of the initial values of  $\mathbf{y}$ . Up to now, we have treated these initial values as free variables and constructed functions of these variables which depended only on the RG transformation. We now need to incorporate the information related to the actual initial values. This calculation depends on the type of models considered. For instance, for a Ising model, one expects

$$y_1 = Y_{1;1}(\beta_c - \beta) + Y_{1;2}(\beta_c - \beta)^2 + \dots, \quad (2.7)$$

and

$$y_l = Y_{l,0} + Y_{l,1}(\beta_c - \beta) + \dots , \quad (2.8)$$

for  $l > 1$ . The  $Y_{l,k}$  are constants that we will evaluate numerically for the HM. The non-leading terms are responsible for the analytical corrections and are usually difficult to resolve numerically. A more complete construction of the initial values in terms of the “bare parameters” used in field theoretical perturbative calculations (with flows starting near the Gaussian fixed point) is in progress [29] but will not be discussed here.

### III. DYSON’S HIERARCHICAL MODEL

In this section, we review the basic facts about the RG transformation of the HM to be used in the rest of the paper and discuss various way to obtain finite dimensional truncations. For more detail, the reader may consult Ref. [21,23] and other papers quoted in the introduction. The energy density of the HM has two parts. One part is non-local (the “kinetic term”) and invariant under a RG transformation. Its explicit form can be found, for instance, in Ref. [21] or in Section II of Ref. [30]. The other part is a sum of local potentials given in terms of a unique function  $V(\phi)$ . The exponential  $e^{-V(\phi)}$  will be called the local measure and denoted  $W_0(\phi)$ . For instance, for Landau-Ginsburg models, the measures are of the form  $W_0(\phi) = e^{-A\phi^2 - B\phi^4}$ , but we can also consider limiting cases such as a Ising measure  $W_0(\phi) = \delta(\phi^2 - 1)$ . Under a block spin transformation which integrates the spin variables in “boxes” with two sites, keeping their sum constant, the local measure transforms according to the integral formula

$$W_{n+1}(\phi) = \frac{C_{n+1}}{2} e^{(\beta/2)(c/4)^{n+1}\phi^2} \int d\phi' W_n\left(\frac{\phi - \phi'}{2}\right) W_n\left(\frac{\phi + \phi'}{2}\right) , \quad (3.1)$$

where  $\beta$  is the inverse temperature (or the coefficient in front of the kinetic term) and  $C_{n+1}$  is a normalization factor to be fixed at our convenience.

We use the Fourier transform

$$W_n(\phi) = \int \frac{dk}{2\pi} e^{ik\phi} \hat{W}_n(k) , \quad (3.2)$$

and introduce a rescaling of  $k$  by a factor  $u/s^n$ , where  $u$  and  $s$  are constants to be fixed at our convenience, by defining

$$R_n(k) \equiv \hat{W}_n\left(\frac{uk}{s^n}\right) , \quad (3.3)$$

In the following, we will use  $s = 2/\sqrt{c}$  with  $c = 2^{1-2/D}$ . This corresponds to the scaling of a massless gaussian field in  $D$  dimensions. Contrarily to what we have done in the past, we will here absorb the temperature in the measure by setting  $u = \sqrt{\beta}$ . With these choices, the RG transformation reads

$$R_{n+1}(k) = C_{n+1} \exp\left[-\frac{1}{2} \frac{\partial^2}{\partial k^2}\right] \left[R_n\left(\frac{\sqrt{c}k}{2}\right)\right]^2 . \quad (3.4)$$



We fix the normalization constant  $C_n$  so that  $R_n(0) = 1$ . For an Ising measure,  $R_0(k) = \cos(\sqrt{\beta}k)$ , while in general, we have to numerically integrate to determine the coefficients of  $R_0(k)$  expanded in terms of  $k$ .

If we Taylor expand about the origin,

$$R_n(k) = 1 + \sum_{l=1}^{\infty} a_{n,l} k^{2l} , \quad (3.5)$$

the finite-volume susceptibility reads

$$\chi_n = -2 \frac{a_{n,1}}{\beta} \left( \frac{2}{c} \right)^n . \quad (3.6)$$

The susceptibility  $\chi$  is defined as  $\chi \equiv \lim_{n \rightarrow \infty} \chi_n$ . For  $\beta$  larger than  $\beta_c$ , the definition of  $\chi$  requires a subtraction (see e. g., Ref. [30] for a practical implementation). In the following, we will only consider the HT phase ( $\beta < \beta_c$ ). The explicit form for  $a_{n+1,l}$  in terms of  $a_{n,l}$  reads

$$a_{n+1,l} = \frac{u_{n,l}}{u_{n,0}} , \quad (3.7)$$

where

$$u_{n,l} \equiv \sum_{i=0}^{\infty} \frac{(-\frac{1}{2})^i (2(l+i))!}{s^{2(l+i)} i! (2l)!} \sum_{p+q=l+i} a_{n,p} a_{n,q} . \quad (3.8)$$

To study the susceptibility not too far from the HT fixed point, we can expand  $\chi$  in terms of  $\beta$ . Since we choose the scaling factor  $u$  so that  $\beta$  is eliminated from the recursion, we find that  $a_{0,l} \propto \beta^l$ . From the form of the recursion, Eq. (3.8), we can see that  $a_{n,l}$  will always have  $\beta^l$  as the leading power in its HT expansion (since  $p+q \geq l$ ). We define the coefficients of the expansion of the infinite-volume susceptibility by

$$\chi(\beta) = \sum_{m=0}^{\infty} b_m \beta^m . \quad (3.9)$$

We define  $r_m \equiv b_m/b_{m-1}$ , the ratio of two successive coefficients, and introduce quantities [19], called the extrapolated ratio ( $\hat{R}_m$ ) and the extrapolated slope ( $\hat{S}_m$ ) which will be used later in a more general context and are defined by

$$\hat{R}_m \equiv m r_m - (m-1) r_{m-1} , \quad (3.10)$$

and

$$\hat{S}_m \equiv m S_m - (m-1) S_{m-1} , \quad (3.11)$$

where

$$S_m \equiv \frac{-m(m-1)(r_m - r_{m-1})}{m r_m - (m-1) r_{m-1}} , \quad (3.12)$$

is called the normalized slope. If we calculate  $\hat{S}_m$  for the HM, we find oscillations illustrated in Refs. [13,14].

The HT expansion can be calculated to very high order, however, due to the amplification of some subleading corrections by the estimators, this is an inefficient way to obtain information about the critical behavior of the HM. In Ref. [23], it was found that one can obtain much better results by neglecting the contribution of the  $a_{n,l}$  when  $l \geq l_{max}$ , with  $l_{max}$  much smaller than the order of the HT expansion. As an example, one can calculate the 1000-th HT coefficient of  $\chi$  with 16 digits of accuracy using only 35 terms in the sum.

This is equivalent to consider the polynomial approximation

$$R_n(k) \simeq \sum_{l=0}^{l_{max}} a_{n,l} k^{2l} , \quad (3.13)$$

for some integer  $l_{max}$ . There remains to decide if one should or not truncate to order  $k^{2l_{max}}$  after squaring  $R_n$ . This makes a difference since the exponential of the second derivative has terms with arbitrarily high order derivatives. Numerically, one gets better results at intermediate values of  $l_{max}$  by keeping all the terms in  $R_n^2$ . In addition, for the calculations performed later, the intermediate truncation pads the “structure constants” of the maps (see sec. V) with about fifty percent of zeroes. A closer look at Section V, may convince the reader that not truncating after squaring is more natural because we obtain correct (in the sense that they keep their value when  $l_{max}$  is increased) structure constants in place of these zeroes. We have thus followed the second possibility where we truncate only once at the end of the calculation. With this choice

$$u_{n,l} \simeq \sum_{i=0}^{2l_{max}-l} \frac{(-\frac{1}{2})^i (2(l+i))!}{(4/c)^{(l+i)} i! (2l)!} \sum_{p+q=l+i} a_{n,p} a_{n,q} . \quad (3.14)$$

Compared to the HT expansion, the initial truncation to order  $l_{max}$  is accurate up to order  $\beta^{l_{max}}$ . After one iteration, we will miss terms of order  $\beta^{l_{max}+1}$  but we will also generate some of the contributions of order  $\beta^{2l_{max}}$  (but not all of them). After  $n$  iterations we generate some of the terms of order  $\beta^{2^n l_{max}}$  as in superconvergent expansions. Rigorous justifications of the polynomial truncation can be found in Ref. [22].

#### IV. A ONE-VARIABLE MODEL

Before attacking the multivariable expansions of the scaling fields, we would like to illustrate the main ideas and study the convergence of series with a simple one variable example which retains the important features: a critical temperature, RG flows going from an unstable fixed point to a stable one, and log-periodic oscillations in the susceptibility.

In order to obtain a simple one-variable model, we first consider the  $l_{max} = 1$  truncation of Eq. (3.14):

$$a_{n+1,1} = \frac{(c/2)a_{n,1} - (3c^2/8)a_{n,1}^2}{1 - (c/2)a_{n,1} + (3c^2/16)a_{n,1}^2} . \quad (4.1)$$

Expanding the denominator up to order 2 in  $a_{n+1,1}$  and using Eq. (3.6), we obtain

$$\chi_{n+1} = \chi_n + \frac{\beta}{4} \left(\frac{c}{2}\right)^{n+1} \chi_n^2 . \quad (4.2)$$

This approximate equation was successfully used in Ref. [23] to model the finite-size effects and was used as the starting point for a study of the scaling field in Ref. [18]. If we expand  $\chi$  (the limit of  $\chi_n$  when  $n$  becomes infinite) in  $\beta$ , and define the extrapolated slope,  $\hat{S}_m$ , as in Eq. (3.11), we see oscillations in Fig. 2 quite similar to those in the HM [13,14]. Using a rescaling discussed in Ref. [18] and the notation  $\xi = c/2$ , the map can be put in the canonical form

$$h_{n+1} = \xi h_n + (1 - \xi) h_n^2 . \quad (4.3)$$

We call this map the “ $h$ -map”. It has a stable fixed point at 0 and an unstable fixed point at 1. We recover the susceptibility as:

$$\chi_n = \frac{h_n}{h_0} \xi^{-n} \quad (4.4)$$

We can expand the map about the unstable fixed point,  $h_n = 1$ . Using the new coordinate  $d_n \equiv 1 - h_n$  and the notation  $\lambda \equiv 2 - \xi$ , we obtain the “dual” map

$$d_{n+1} = \lambda d_n + (1 - \lambda) d_n^2 , \quad (4.5)$$

with the starting value  $d_0 = 1 - \beta/\beta_c$ . We call this map the “ $d$ -map” and we can think of  $d$  as being the distance to the critical point. We can construct a function  $d$  such that  $d(y_n) \equiv d_n$  by plugging an expansion in  $y_n$  into the equation

$$d(\lambda y_n) = \lambda d(y_n) + (1 - \lambda) d^2(y_n) . \quad (4.6)$$

Similarly, we can construct the inverse series and obtain  $d(y_n)$ . This allows us construct  $d_n$  in terms of  $d_0$ :

$$d_n = y^{-1}(\lambda^n y(d_0)) . \quad (4.7)$$

Because of the duality between our two maps, we can easily reproduce all of the above results of the  $d$ -map for the  $h$ -map and express  $h_n$  in terms of a HT scaling field  $\tilde{y}_n$ .

We now turn to the three steps. Note that step 3 is not necessary: the knowledge of  $y(d_0)$  provides the initial value of  $y$  as a function of  $\beta$ . Step 1 is straightforward. As shown in Ref. [18], in the infinite  $n$  limit,

$$\chi = \frac{\tilde{y}_0}{h_0} = \frac{\tilde{y}(h_0)}{h_0} . \quad (4.8)$$

The only difficult part is step 2. The susceptibility can be written as

$$\chi = \frac{\Theta}{(1 - d_0)(y(d_0))^\gamma} . \quad (4.9)$$

with the RG invariant  $\Theta \equiv \tilde{y}_0 y_0^\gamma$ . Due to the discrete nature of our RG transformation,  $\Theta$  is not exactly a constant. If expressed in terms of  $\ln(y_0)$ ,  $\Theta$  is a periodic function of period

$\ln \lambda$ . However, for  $\lambda$  not too close to 2, the non-zero Fourier modes are very small. Note also that the apparent singularity when  $d_0 \rightarrow 1$  is exactly canceled by  $y(d_0)^\gamma$  by virtue of Eq. (4.11) discussed below. We now give empirical results concerning the large order behavior of the expansions of  $y(d)$ ,  $\tilde{y}(h)$  and their inverses.

We first consider  $d(y) = y + \sum_{l=2}^{\infty} s_l y^l$ . For all tested values of  $1 < \lambda < 2$ , we obtained very good linear fits of  $\ln |s_{l-1}/s_l|$  versus  $\ln(l)$ , for  $l$  large enough. Thus for large  $l$ , the coefficients obey the approximate rule

$$\left| \frac{s_l}{s_{l+1}} \right| \simeq C l^k, \quad (4.10)$$

where we find that  $C$  is always of order 1 (in fact,  $0.9 < C < 1$ ) and  $0 < k < 1$ . Using iteratively this formula, we find that the coefficients decrease like  $C^{-l}(l!)^{-k}$  and consequently the  $d(y)$  should be an entire function. The numerical values of  $k$  are given in Fig. 3.

We then consider  $h(\tilde{y})$  and again examine the ratios of successive coefficients,  $|s_l/s_{l+1}|$ . We find the ratios flatten to constant values, for large enough  $l$ , indicating a finite radius of convergence. The radius get smaller and vanish as  $\xi$  approaches zero as shown in Fig. 4. Note that for any value of  $\xi$  tried, we found good evidence that  $\lim_{n \rightarrow \infty} \hat{S}_n = -1.5$ , indicating a  $(\tilde{y} - \tilde{y}_c)^{1/2}$  behavior. This is consistent with the existence of a quadratic minimum for the inverse function discussed below.

We now turn to the inverse functions starting with  $y(d)$ . As  $d \rightarrow 1$ , we reach the HT fixed point and we expect the convergence of the series to break down in this limit. We find empirically from the analysis of ratios that for all  $1 < \lambda < 2$ ,  $y(d)$  converges in the region  $0 < d < 1$ . The analysis of the extrapolated slope for various  $\lambda$  gives convincing evidence that the main singularity has the form

$$y(d) \sim (1 - d)^{-1/\gamma}. \quad (4.11)$$

This can be seen with short series when  $\lambda$  is close to one and requires larger and larger series as  $\lambda$  gets close to 2. Illustration of these properties for a particular value of  $\lambda$  are shown in Figs. 7 and 8 where the estimators are compared with those of the HM.

Finally, we discuss  $\tilde{y}(h)$  which can be seen as a high-temperature expansion. We found clear evidence that the ratio of coefficients  $t_l/t_{l+1}$  approaches 1 for large  $l$ . For smaller values of  $\xi$ , it takes larger order to reach this limit. A detailed study shows that if we continue  $\tilde{y}(h)$  for negative values of  $h$  using the series expansion, the function develops a quadratic minimum at some negative value of  $h$ . The absolute value of  $\tilde{y}$  at that value of  $h$ , in all examples studied, reproduces accurately the radius of convergence of the inverse function. As one may suspect by looking at Fig. 2, the analysis of the extrapolated slope is intricate. However, if we calculate enough terms and if  $\lambda$  is not too close to 2, we get approximate results which are consistent with a main singularity of the form

$$\tilde{y}(h) \sim (1 - h)^{-\gamma}. \quad (4.12)$$

For instance, just by looking at the asymptotic behavior of Fig. 2, one can see that  $\gamma \simeq 1.4677$ , as expected, with errors of the order  $10^{-4}$ . It is interesting to note the duality [18] between Eqs. (4.11) and (4.12).

All the results concerning the convergence and the singularities have a simple interpretation. The finite radius of convergence of  $y$  and  $\tilde{y}$  is due to the other fixed point which cannot

be located inside the domain of convergence. In this simple example there are exactly two fixed points in the complexification of the map and this concludes the discussion. On the other hand, the finite radius of  $h$  is due to a minimum of  $\tilde{y}$  at negative values of  $h$  while such a minimum does not appear for  $d$ .

As we have seen above,  $\tilde{y}_n y_n^\gamma$  is independent of  $n$ . We can thus pick  $n$  such that we are just in the crossover region and *both* expansions have a reasonable chance to be accurate. In order to test the accuracy of the approximations  $y_{app}(d)$  (series expansion up to a certain order) for various  $n$ , we have prepared an empirical sequences of  $d_n$  starting with  $d_0 = 10^{-8}$ . We have then tested the scaling properties by calculating

$$D_n = |[y_{app}(d_n)/(y_0 \lambda^n)] - 1| , \quad (4.13)$$

where  $y_0$  was calculated with 16 digits of accuracy by using enough terms in the expansion of  $y(d_0)$ . For double precision calculations, optimal approximations are those for which  $D_n \simeq 10^{-16}$ . For such approximation, the scaling is as good as it can possibly be given the accuracy of  $y_0$ . Indeed, due to the peculiar way numerical errors propagate [31], one does not reach exactly the expected level  $10^{-16}$ . We can define a similar dual quantity by replacing  $d$  by  $h$  and  $y$  by  $\tilde{y}$ . In this case,  $\tilde{y}_0$  is estimated with the same accuracy as  $y_0$  by stabilizing  $\tilde{y}(h_n)/\xi^n$ , for large enough  $n$ .

We have performed this calculation for  $\lambda = 1.1, 1.5$  and  $1.9$ . The conclusions in the three cases are identical. For  $n$  large enough, the  $D_n$  of  $y$  starts increasing from  $10^{-16}$  until it saturates around 1. By increasing the number of terms in the expansion, we can increase the value of  $n$  for which we start losing accuracy. Similarly, for  $n$  low enough, the  $D_n$  of  $\tilde{y}$  starts increasing etc... We want to know if it is possible to calculate enough terms in each expansion to get scaling with some desired accuracy for both functions. The answer to this question is affirmative according to Fig. 5 for  $\lambda = 1.5$ . One sees, for instance, that with 10 terms in each series, we have scaling with about 1 part in 1000 near  $n = 45$  for both expansions. The situation can be improved. For 70-70 expansions, an optimal accuracy is reached from  $n = 44$  to 46. For the other values of  $\lambda$  quoted above, similar conclusions are reached, the only difference being the optimal values of  $n$ .

Another evidence for overlapping convergence is that we can stabilize the RG invariant  $\Theta$  for a certain range of  $y_n$ . To evaluate  $\Theta$ , we use the series expansions for  $\tilde{y}$  and  $d$ , cutting each off at some order:

$$\tilde{y}(1 - d(y)) \simeq \sum_{i=1}^{\tilde{m}} t_i (1 - \sum_{j=1}^m s_j y^j)^i , \quad (4.14)$$

where  $s_l$  and  $t_l$  are the  $l$ th coefficients in the  $d$  and  $\tilde{y}$  series, respectively. We have found that, given a fixed value of  $m + \tilde{m}$ , the most accurate values for  $\Theta$  are obtained when  $m \simeq \tilde{m}$ . In Fig. 6, we show  $\Theta$  calculated by keeping 50 terms each in the expansions for  $y$  and  $\tilde{y}$ . The result is plotted against  $\ln(y)$ . We used  $\xi = 0.1$ , which makes the oscillations much larger than, for example, near to  $\xi = 2^{-2/3}$ . Near the fixed points, we need more terms in the appropriate series to get accurate results.

We can study the oscillation we see in  $\Theta$  by looking at its Fourier expansion. Since  $\Theta$  is periodic in  $\ln y_0$ , we can express

$$\Theta(y_0) = y_0^\gamma \tilde{y}(1 - d(y_0)) = \sum_p a_p e^{ip\omega \ln y_0} , \quad (4.15)$$

where  $\omega \equiv 2\pi/\ln \lambda$ . The coefficients are given as

$$a_p = \frac{1}{\ln \lambda} \int_{y_a}^{\lambda y_a} y^{\gamma-1-ip\omega} \tilde{y}(1-d(y)) dy , \quad (4.16)$$

As an example, we calculated  $a_0$  for  $\xi = 0.1$  where the oscillations are not too small. The choice of the interval of integration can be inferred from Fig. 6. If we had infinite series, the function would be exactly periodic. For finite series, we see that  $y_a$  cannot be too large or too small. For intermediate values, we obtain  $a_0 \simeq 6.06676$ . Proceeding similarly, we were able to resolve the next two Fourier modes. For reference, the magnitude of  $a_2$  is about  $2 \times 10^{-10}$ . Using  $\Theta \simeq a_0$  together with Eq. (4.9), we obtain the leading amplitude together with the analytical corrections coming from the nonlinear terms in  $y(d)$ .

## V. SCALING FIELDS IN THE HIERARCHICAL MODEL

### A. Construction of the scaling fields

For notational convenience, we first rewrite the unnormalized recursion given in Eq. (3.14), using the “structure constants”:

$$u_{n,\sigma} = \Gamma_{\sigma}^{\mu\nu} a_{n,\mu} a_{n,\nu} , \quad (5.1)$$

with

$$\Gamma_{\sigma}^{\mu\nu} = \begin{cases} (c/4)^{\mu+\nu} \frac{(-1/2)^{\mu+\nu-\sigma} (2(\mu+\nu))!}{(\mu+\nu-\sigma)!(2\sigma)!} & , \quad \text{for } \mu + \nu \geq \sigma \\ 0 & , \quad \text{otherwise} . \end{cases} \quad (5.2)$$

These zeroes can be understood as a “selection rule” associated with the fact that  $a_{n,l}$  is of order  $\beta^l$  as explained in Section III. If we follow the truncation procedure explained in Section III, the indices simply run over a finite number of values. We use “relativistic” notations. Repeated indices mean summation. The greek indices  $\mu$  and  $\nu$  go from 0 to  $l_{max}$ , while latin indices  $i, j$  go from 1 to  $l_{max}$ . Obviously,  $\Gamma_{\sigma}^{\mu\nu}$  is symmetric in  $\mu$  and  $\nu$ . By construction,  $a_{n,0} = 1$  and we can write the normalized recursion in the form:

$$a_{n+1,l} = \frac{\mathcal{M}_l^i a_{n,i} + \Gamma_l^{ij} a_{n,i} a_{n,j}}{1 + \mathcal{M}_0^i a_{n,i} + \Gamma_0^{ij} a_{n,i} a_{n,j}} , \quad (5.3)$$

with  $\mathcal{M}_{\eta}^i = 2\Gamma_{\eta}^{0i}$ .

We then expand the basic map of Eq. (5.3) about the two fixed points of interest, choosing coordinates such that the matrix associated with the linearized RG transformation becomes diagonal. This matrix is not symmetric and the relations of orthogonality and completeness are left invariant under rescaling of any right eigenvector by a nonzero constant together with a rescaling of the corresponding left eigenvector by the inverse. In the following, we will fix this ambiguity by requiring, in analogy with Section IV that the “other” fixed point (i.e. the one not located at the origin by construction) be at  $(1, 1, \dots)$  in the new coordinates.

The HT fixed point is at the origin of the coordinates in Eq. (5.3) and all we need to do is diagonalizing the linear form  $\mathcal{M}_i^j$ . This is quite simple because it is of the upper

triangular form. The eigenvalues are just the diagonal terms. From Eq. (5.2), one sees that  $l$ th diagonal term is given as

$$\tilde{\lambda}_r = 2(c/4)^r . \quad (5.4)$$

This spectrum was obtained in Lemma 3.3 of Ref. [21] with a different method. This spectrum has a simple interpretation which will be discussed below. The upper diagonal form implies that the  $l$ -th right eigenvector has only its  $l$  first entries non-zero. This means that if we truncate to  $a_{l_{max}}$ , we are simply truncating to a subspace spanned by the first  $l_{max}$  eigenvectors. This is an interesting reinterpretation of the original polynomial truncation which can be applied for other models. Introducing new coordinates  $h_l$ , so that  $a_{n,l} = \tilde{\psi}_l^r h_{n,r}$  with  $\tilde{\psi}$  the matrix of right eigenvectors, the RG transformation has the form

$$h_{n+1,r} = \frac{\tilde{\lambda}_r h_{n,r} + \tilde{\Delta}_r^{pq} h_{n,p} h_{n,q}}{1 + \tilde{\Lambda}^p h_{n,p} + \tilde{\Delta}_0^{pq} h_{n,p} h_{n,q}} . \quad (5.5)$$

Note that the form of the eigenvectors guarantees that  $h_{n,l}$  is of order  $\beta^l$ . This can be seen by inverting the linear change of variable using the matrix of left eigenvectors. Due to the upper-diagonal form of the linear transformation, the second left eigenvector has its first entry equal to zero, the third its first two entries etc... .

Near the nontrivial fixed point, we first use accurate values of the fixed point [25] to bring the fixed point at the origin. The eigenvectors are then calculated numerically using truncated forms of the linearized RG transformation. There is no exact closure as in the HT case, however the first eigenvalues stabilize rapidly when  $l_{max}$  increases. There is only one eigenvalue larger than 1. For instance the numerical values for  $c = 2^{1/3}$  are  $\lambda_1 = 1.42717 \dots$ ,  $\lambda_2 = 0.85941 \dots$ . A more complete list is given in Ref. [24]. In summary, we can choose a system of coordinate  $d_l$  where the unstable fixed point will be at the origin of the coordinate and the HT fixed point at  $(1, 1, \dots)$ , and such that the RG transformation has the form

$$d_{n+1,r} = \frac{\lambda_r d_{n,r} + \Delta_r^{pq} d_{n,p} d_{n,q}}{1 + \Lambda^p d_{n,p} + \Delta_0^{pq} d_{n,p} d_{n,q}} , \quad (5.6)$$

We can express canonical coordinates (linear scaling fields) in terms of the nonlinear scaling fields:

$$d_{n,r} = \sum_{i_1, i_2, \dots} s_{r, i_1 i_2 \dots} y_{n,1}^{i_1} y_{n,2}^{i_2} \dots , \quad (5.7)$$

where the sums over the  $i$ 's run from 0 to infinity in each variable and  $y_{n,l} = \lambda_l^n y_{0,l}$ . Using the notation  $\mathbf{i} = (i_1, i_2 \dots)$  and the product symbol, we may rewrite the expansion as

$$d_{n,r} = \sum_{\mathbf{i}} s_{r,\mathbf{i}} \prod_m y_{n,m}^{i_m} \quad (5.8)$$

Using the transformation law for the scaling fields, we have

$$d_{n+1,r} = \sum_{\mathbf{i}} s_{r,\mathbf{i}} \prod_m (\lambda_m y_m)^{i_m} . \quad (5.9)$$

Each constant term,  $s_{r,0,0,\dots}$ , is zero, as the scaling fields vanish at the fixed point. From Eq. (5.6), we see that all but one of the linear terms are zero for each value of  $r$ . The remaining term is the one proportional to the  $r$ th scaling variable. We take these coefficients to be 1, so that the  $d_{n,r} \simeq y_{n,r}$  for small  $y_{n,r}$ . For the higher-order terms, we obtain the recursion

$$s_{r,i} = \frac{\sum_{j+k=i} (\Delta_r^{pq} s_{p,j} s_{q,k} - s_{r,j} \prod_m \lambda_m^{j_m} \Lambda^p s_{p,k}) - \sum_{j+k+l=i} s_{r,j} \prod_m \lambda_m^{j_m} \Delta_0^{pq} s_{p,k} s_{q,l}}{(\prod_m \lambda_m^{i_m} - \lambda_r)} . \quad (5.10)$$

The calculation can be organized in such way that the r. h. s. of the equations are already known. This will be the case for instance if we proceed order by order in  $\sum_q i_q$ , the degree of non-linearity. This expansion may have small denominator problems. However, as discussed in the introduction, using numerical values of the eigenvalues as calculated in [24], we did not find spectacular cancellations between the two terms entering the denominator.

We can likewise expand each  $h_{n,r}$  in terms of scaling fields  $\tilde{y}_{n,1}, \tilde{y}_{n,2}, \dots$ . The derived recursions are identical in form to those derived above. From Eq. (5.4), one sees that the denominator will vanish for some equations. This question is discussed in [26] where it is shown that to all order relevant for the following calculation, a zero denominator always comes with a zero numerator.

One can likewise find expansions of the scaling fields in terms of the canonical coordinates, by setting

$$y_{n,r} = \sum_{\mathbf{i}} u_{r,\mathbf{i}} \prod_m d_{n,m}^{i_m} , \quad (5.11)$$

and requiring that when  $\mathbf{d}_n$  is replaced by  $\mathbf{d}_{n+1}$ , the function is multiplied by  $\lambda_r$ . Since  $\mathbf{d}_{n+1}$  has a denominator, it needs to be expanded for instance in increasing order of non-linearity. A simple reasoning shows that exactly the same small denominators as in Eq. (5.10) will be present in these calculations. The same considerations applies for  $\tilde{y}$ .

## B. Practical implementation

We have calculated an empirical series of  $a_{n,l}$  with  $c = 2^{1/3}$ , an initial Ising measure and  $\beta = \beta_c - 10^{-8}$ . Detail relevant for this calculations can be found in Refs. [23,24,31]. The calculations have been performed with  $l_{max} = 30$ , a value for which at the  $\beta$  considered, the errors due to the truncation are of the same order as those due to the numerical errors. These errors are small enough to allow a determination of the susceptibility with seven significant digits if we use double precision.

We now discuss the flow chronologically. Our choice of  $\beta$  (close to  $\beta_c$ ) means that we start near the stable manifold. After about 25 iterations, we start approaching the unstable fixed point and the linear behavior  $d_{n+1,l} \simeq \lambda_l d_n$  becomes a good approximation. During the next 20 iterations, the irrelevant variables die off at the linear rate and at the same time the flow moves away from the fixed point along the unstable direction, also at the linear rate. At  $n = 47$  we are in good approximation on the unstable manifold and  $d_{n,2}$  becomes proportional to  $d_{n,1}^2$ . In other words, the non-linear terms are taking over. At this point, we can approximate the  $d_{n,l}$  as functions of  $y_1$  *only*:  $d_{n,l} \simeq d_l(\lambda_1^n y_1, 0, 0, \dots)$ . This



approximation is consistent in the sense that if  $y_2 = 0$  at  $n = 0$  then it is also the case for all positive  $n$ .

We have calculated  $d_l(y_1, 0, 0, \dots)$  up to order 80 in  $y_1$  using Eq. (5.10). There cannot be any small denominators in this restricted case. We have then inverted  $d_1$ , now a function of  $y_1$  only, to obtain  $y_1(d_1)$ . Given the empirical  $d_{n,1}$  we then calculated the approximate  $y_{n,1}$  and then used the other functions  $d_l(y_1)$  (with  $l \geq 2$ ) calculated before to “predict”  $d_{n,l}$ . Comparison with the actual numbers were good in a restricted range. For  $n = 49$ , the relative errors were less than a percent. They kept decreasing to less than one part in 10,000 for  $n = 54$  and then increased again. It will be shown later that this corresponds to the fact that when  $y_1$  becomes too large (a value of approximately 3.7 first exceeded at  $n = 57$ ), the series expansion of  $d_1$  seem to diverge, unlike the one-variable model for which  $d(y)$  is an entire function.

The quality of the approximation between  $n = 45$  and  $n = 55$  can be improved by treating  $y_2$  perturbatively. We have expanded

$$d_l(y_1, y_2, 0, \dots) \simeq d_l^{(0)}(y_1, 0, 0, \dots) + y_2 d_l^{(1)}(y_1, 0, 0, \dots) , \quad (5.12)$$

with  $d_l^{(1)}$  up to order 30 in  $y_1$ . This allows us to obtain the first order expression:

$$\tilde{y}_1(\mathbf{h}(\mathbf{d}(y_1, y_2, 0, \dots))) \simeq G(y_1) + y_2 H(y_1) . \quad (5.13)$$

Note that expansions at *both* fixed points are involved (one for  $\tilde{y}_1$  and one for  $\mathbf{d}$ ) in this equation. When finite series are used, the approximation will only be valid in the crossover region. Near  $n = 55$ , the presence of the HT fixed point starts dominating the flow but we are still far away from the linear regime. We have taken these non-linear effects in  $\tilde{y}_1(\mathbf{h})$  into account by calculating it up to order 11 in  $\beta$ . This is a multi-variable expansion. Recalling the discussion about the HT expansion in Section III and the properties of the eigenvectors of the linearized RG transformation about the HT fixed point, we can count the number of terms at each order in  $\beta$ . At order two, we have  $h_1^2$  and  $h_2$ , but since the linear transformation is diagonalized,  $h_2$  will only appear in  $\tilde{y}_2(\mathbf{h})$  with coefficient 1. It is easy to see that at order  $l$ , one needs to determine  $p(l) - 1$  coefficients, where  $p(l)$  is the number of partitions of  $l$ . It has been known from the work of Hardy and Ramanujan that

$$p(l) \sim \frac{\exp(\pi\sqrt{2l/3})}{4\sqrt{3}l} . \quad (5.14)$$

It seems thus difficult to get very high order in this expansion. In order to fix the ideas, there are 41 terms at order 11, 489 at order 20 and 13,848,649 at order 80.

As we will explain below, the expansion up to order 11 has a sufficient accuracy to be used starting at  $n = 55$ . It also provides optimal (given our use of double precision) results for  $n \geq 60$ . As  $n$  increases beyond 60, one can see the effect of each order disappear one after the other as discussed in VD. Finally, the linear behavior becomes optimal near  $n = 130$ . This concludes our chronological discussion.

### C. Step 1

From Eqs. (3.6) and remembering that we have absorbed  $\beta$  in the  $a_n$ , we obtain

$$\chi_n = -(2/\beta)\tilde{\psi}_1^r h_{n,r}(2/c)^n , \quad (5.15)$$

where  $\tilde{\psi}$  is the matrix of right eigenvectors. For  $n$  large enough, the linear behavior applies and the  $h_{n,r}$  get multiplied by  $2(c/4)^r$  at each iteration. In the large  $n$  limit, only the  $r = 1$  term survives and consequently,

$$\chi = -(2/\beta)\tilde{\psi}_1^1 \lim_{n \rightarrow \infty} h_{n,1}(2/c)^n . \quad (5.16)$$

Using the same method as in the one-variable model, we can in the limit replace  $h_{n,1}$  by  $\tilde{y}_{n,1}$  and obtain

$$\chi = -(2/\beta)\tilde{\psi}_1^1 \tilde{y}_{0,1} . \quad (5.17)$$

For reference, in the case  $c = 2^{1/3}$  and with the normalization of the eigenvectors discussed above,  $\tilde{\psi}_1^1 \simeq -0.564$ . Also note that since for all  $l$ ,  $0 < \tilde{\lambda}_l < 1$ , all other monomials in the  $\tilde{y}_l$  go to zero faster than  $\tilde{y}_1$ .

One can calculate the subtracted  $2q$ -point function following the same procedure. As shown in [23,30], they can be expressed in terms of  $a_{q,n}$  and higher powers of the  $a_{n,l}$  with  $l < q$ . Following the procedure described above, these quantities can then reexpressed in terms of  $\tilde{y}$ . We need to identify the leading term in this expansion. By rescaling  $(-1)^q(2q)!a_{q,n}$  by  $(4/c)^n$  we obtain the average value of the  $2q$ -th power of the main spin (sum of the  $2^n$  spin variables  $\phi_x$ ). In the symmetric phase, this quantity scales like  $2^{qn}$  when  $n$  increases. However, the subtracted version of this quantity (which is generated by the free energy) is expected to scale like  $2^n$ . In other words, if we assume that the free energy density is finite

$$a_{q,n} - (\text{subtractions}) \propto [2(c/4)^q]^n . \quad (5.18)$$

One clearly recognizes the spectrum of Eq. (5.4) and expects that the leading term is

$$a_{q,n} - (\text{subtractions}) \propto \tilde{y}_{n,q} . \quad (5.19)$$

In order to prove this conjecture by direct algebraic methods, one needs to show that the the non-linear terms which scale faster than  $\tilde{y}_{n,q}$  are canceled by the subtraction. For instance for the subtracted four-point function and  $c = 2^{1/3}$ ,  $\tilde{\lambda}_1^2 > \tilde{\lambda}_2$  and  $\tilde{\lambda}_1^3 > \tilde{\lambda}_2$ . We have checked that the corresponding terms  $(\tilde{y}_1)^2$  and  $(\tilde{y}_1)^3$  disappear with the subtraction. We have conducted similar checks for the 6 and 8 point functions [29] and found similar cancellations. It should be noted that a rigorous proof that the mechanism works in general, would imply the finiteness of the free energy density and hyperscaling (as defined in [30]). The practical calculation of the subtracted quantities is made difficult by the fact that as  $n$  increases, the “signal” becomes much smaller than the “background” (the unsubtracted part). This requires the use of adjustable precision arithmetic. In the following, we will only discuss the 2 point function (susceptibility).

## D. Step 2

We rewrite the susceptibility as

$$\chi \simeq (1.127853/\beta)\Theta(y_{0,1})^{-\gamma} , \quad (5.20)$$

with the RG invariant  $\Theta \equiv \tilde{y}_{0,1}y_{0,1}^\gamma = \tilde{y}_{n,1}y_{n,1}^\gamma$ . We first constructed  $y_1(d_1)$  by neglecting the effects of the irrelevant directions, as explained in subsection VB. In order to provide a comparison, we have calculated the same  $y(d)$  for the one-variable model with  $\lambda = 1.2573$ . In the following, we call this model the “simplified model” (SM). For this special value of  $\lambda$ , the critical exponents  $\gamma$  of the two models coincide with five significant digits. We have good evidence that both series have a radius of convergence 1 as indicated by the extrapolated ratio defined in Eq. (3.10) reaching 1 at an expected rate (Fig. 7). Similarly, their extrapolated slopes seem to converge to the same value  $1/\gamma - 1 \simeq -0.23026 \dots$  as shown in Fig. 8. In conclusion, the function  $y(d)$  for the SM is a reasonably good model to guess the asymptotic behavior of  $y_1(d_1)$ . Remembering the explanations of Section IV, this indicates the absence of other fixed points in the vicinity of the unstable fixed point.

For the inverse function  $d_1(y_1)$ , the situations more complicated as shown in Fig. 9. The quantity plotted in this figure will be used to discriminate between a finite and an infinite radius of convergence. If  $|b_m| \sim R^{-m}$  as for a radius of convergence  $R$ , then we have  $\ln(|b_m|)/m \sim -\ln(R) + A/m$  for some constant  $A$ . On the other hand, if  $|b_m| \sim (m!)^{-\alpha}$  as for an infinite radius of convergence, then we have  $\ln(|b_m|)/m \sim -\alpha(\ln(m) - 1)$ . In the following, we will compare fits of the form  $A_1 + A_2/m$  and  $B_1 \ln(m) + B_2$ . We first consider the case of SM, where according to our study in Section IV, expect an infinite radius of convergence. This possibility is highly favored as shown in Fig. 10. One sees clearly that the solid line is a much better fit. The chi-square for the solid line fit is 200 times smaller. In addition  $B_1 \simeq -B_2$  as expected.

The analysis for the HM is more delicate. One observes periodic “dips” in Fig. 9 which make the ratio analysis almost impossible. We have thus only considered, the “upper envelope” by removing the dips from Fig. 9. The fit represents an upper bound rather than the actual coefficients. The fits of the upper envelope are shown in Fig. 11. The possibility of a finite radius of convergence is slightly favored, the chi-square being 0.4 of the one for the other possibility. Also, the second fit does not have the  $B_1 \simeq -B_2$  property. From  $A_1 \simeq -1.32$ , we estimate that the radius of convergence is about 3.7. This means that if we want to write some analytical formula for the flows by first calculating the initial values of the scaling fields and then calculating  $\mathbf{d}$  at successive iterations by using their expression in terms of the scaling fields, we will have to switch variables in the crossover region.

As explained above, the approach of the HT fixed point is intrinsically a multivariable problem. For this reason, the calculation of  $D_n$ , defined in Eq. (4.13), that tests the quality of scaling, will be our main tool of analysis. In the following, we limit the discussion to  $\tilde{y}_1(\mathbf{h})$  which enters in the susceptibility. We have calculated  $\tilde{y}_1(\mathbf{h})$  in terms of 11 variables, up to order 11 in  $\beta$ . As in section IV, we will use an empirical series  $a_{n,l}$ , calculate the corresponding  $h_{n,l}$  and plug them in the scaling fields and check the scaling properties. This empirical series was calculated with an initial Ising measure and  $\beta = \beta_c - 10^{-8}$  (see Ref. [24]). Again we define a quantity  $D_n$  as in Eq. (4.13) which is very small when we have good scaling and increases when the approximation breaks down. The results are shown in Fig. 12 for successive orders in  $\beta$ . The solid line on the right is the linear approximation. It becomes optimal near  $n = 130$ . The next line (dashes) is the second order in  $\beta$  expansion. It becomes optimal near  $n = 90$ . Each next order gets closer and closer to be optimal near  $n = 60$ . The last curve on the left is the order 9 approximation. It is hard to resolve the next two approximations on this graph.

The asymptotic value is stabilized with 16 digits and one may wonder why we get only scaling with 14 or 15 digits in Fig. 12. The reason is that we use empirical data and that numerical errors can add coherently as explained in Ref. [31]. This can be seen directly by considering the difference between two successive values of  $D_n$ . A detailed analysis shows that the numerical errors at each step tend to be negative more often than positive, and consequently there is a small “drift” which affects the last digits.

We can now look at the  $D_n$  defined as in Eq. (4.13) for  $y_1$  and  $\tilde{y}_1$  together in Fig. 13. If we use an expansion of order 5 in  $\beta$  for  $\tilde{y}$  and of order 10 in  $d_1$  for  $y_1$ , we can get scaling within a few percent for both variables at  $n = 54$ . We can go below 1 part in 1000, with an expansion of order 11 in  $\beta$  and order 80 in  $d_1$ . At this point, the main problem is that the effects of the subleading correction makes the scaling properties *worse* when  $n \leq 57$  and  $n$  decreases. One can improve the scaling properties by taking the effects of  $y_2$  into account. A detailed study shows that one can estimate the subleading effects between  $n = 40$  and  $n = 45$  as

$$\frac{y_1(d_{n,1})}{\lambda_1^n} \simeq 7.2778 \times 10^{-9} + 3.2 \times 10^{-9} \times \lambda_2^n \quad (5.21)$$

It is thus possible to get a function scaling better by subtracting these correction. This improve the scaling properties by almost one order of magnitude near  $n = 54$  and by almost two order of magnitude near  $n = 45$ . From Fig. 13, we see that the combined scaling is optimal near  $n = 54$  which corresponds to an approximate value of 2 for  $y_1$ .

Using Eq. (5.12), we can take into account the first order correction in  $y_2$ . After simple manipulations, we can rewrite the RG invariant as

$$\Theta \simeq C_1 + C_2 y_{2,0} (y_{1,0})^\Delta, \quad (5.22)$$

with  $C_1 = G(y_1)y_1^\gamma$  and  $H(y_1)y_1^{\gamma-\Delta}$ . The functions  $G$  and  $H$  are defined by Eq. (5.13). They rely on *both* expansions used and consequently they are only valid in a crossover region. Using explicit forms of  $C_1$  and  $C_2$  as a function of  $y_1$ , we observe a plateau for each function which are shown in Fig. 14. Using the flattest part of the plateau to estimate the constant we obtain  $C_1 \simeq 1.46416$  and  $C_2 \simeq 1.663$ . Note that these two numbers are dependent of the choice of the scales for the scaling fields, but independent of the initial conditions. Consequently, if everybody agreed on the scales, these quantities could be called universal.

### E. step 3

There remains to estimate the initial values of the  $y_1$  and  $y_2$ . This step will done numerically from empirical values of  $\mathbf{d}_n$ . First, we obtain a rough estimate of  $y_{2,n}$  from  $d_{2,n}$  at values of  $n$  where the linear approximation is good. Plugging this value in Eq. (5.12) for  $l = 1$ , and inverting to get  $y_{n,1}$  as a function of  $d_{n,1}$ . Dividing by  $\lambda_1^n$  we get an estimated value of  $y_{0,1}$  with a plateau of about 10 iterations where the value is stabilized with 6 digits. Repeating for various temperatures we were able to determine the leading coefficient in Eq. (2.7):  $Y_{1,1} \simeq 0.72782$ . Using Eq. (5.12) but for  $d_2$ , together with our previous estimates of  $y_{1,n}$ , we obtain  $Y_{2,0} \simeq -0.565$ . Subleading coefficients are difficult to resolve because  $2\Delta \sim 1$  and the nonlinear contributions in  $y_2$  are of the same order as the analytical corrections.

This concludes our approximate treatment of step 3. Using Eqs. (5.20) and (5.22) we obtain the usual parametrization of the susceptibility of Eq. (1.1) with  $A_0 \simeq 2.1162$  and  $A_1 \simeq -1.196$  in very good agreement with a fully numerical determination of these amplitudes [24].

## VI. CONCLUSIONS

In summary, we have shown with two examples that the 3 steps advocated in Section II lead to an accurate determination of the leading and subleading critical amplitudes. We provided numerical evidence that the formal expansions of the scaling fields associated with the HT and unstable fixed point have reasonable convergence properties and scale properly in overlapping domains. The determination of the initial values of the scaling fields associated with the unstable fixed point (third step) have been obtained numerically in the case of an initial Ising measure. Putting everything together, we were able to confirm numerical results obtained earlier.

Analytical methods are now being used [29] to consider initial measures of the Landau-Ginzburg type in the vicinity of the Gaussian fixed point. For such initial measures, we can use perturbation theory in the quartic (or higher orders) coupling constant to construct the scaling fields associated with the Gaussian fixed point. Interestingly, one could use some of the methods developed here to interpolate between the Gaussian fixed point and the unstable fixed point. The completion of this task will allow us to give analytical expressions for the renormalized quantities in terms of the bare ones, which is the notoriously difficult problem that has to be faced by a field theorist. We are planning to extend the calculations performed here, to higher order derivatives of the free energy with a non-zero magnetic field and check explicitly amplitudes relations appearing in the literature [32–34]. Another interesting question that could be addressed within this context is the crossover from classical to critical behavior [7,9,10]. The completion of these projects will provide a detailed comparison between general RG expectations and their practical realization for the HM.

The hierarchical approximation used in this article has allowed us to calculate large order expansions for the scaling fields. The fact that the general ideas advocated have worked properly means that one should now attempt to apply them to nearest neighbor models where similar calculations would be more time consuming. The examples we have in mind are spin models in three dimensions and asymptotically free theory such as the  $O(N)$  spin models in two dimensions or lattice gauge theory in four dimensions. In all cases, there exists some advanced technology for the weak and strong coupling expansions but the question of the interpolation has only been studied with the Monte Carlo method [6,8].

We expect that some of the simple features found in the study of the HT fixed point of the HM will generalize to nearest neighbor models. First, the fact that the HT scaling fields are linearly related to the successive derivatives of the free energy. Second, the fact that the restriction to a finite number of eigenvectors of the linearized RG transformation near the HT fixed point can be used to obtain improved HT expansions such as the polynomial truncation used above. However, the most difficult task remains a construction of the unstable fixed point and the RG flows in its vicinity, with a control comparable to the case the hierarchical model. This is a challenging problem for the future.

## ACKNOWLEDGMENTS

This research was supported in part by the Department of Energy under Contract No. FG02-91ER40664. Y. M. thanks the Aspen Center for Physics, where discussions have motivated part of this work and where part of this manuscript was written.

## REFERENCES

- [1] V. Privman, P. Hohenberg and A. Aharony, in *Phase Transitions and Critical Phenomena*, v. 14, C. Domb and J. Lebowitz Editors (Academic Press, New York, 1991), and references therein.
- [2] H. Poincaré, *Les Methodes Nouvelles de la Mecanique Celeste* (Gauthier-Villars, Paris, 1892).
- [3] V. Arnold, *Geometrical Methods in the Theory of Ordinary Differential Equations* (Springer-Verlag, New York, 1988).
- [4] F. Wegner, Phys. Rev. B **3**, 4529 (1972).
- [5] J. Cardy, *Scaling and Renormalization in Statistical Physics* (Cambridge University Press, Cambridge, 1996).
- [6] A. Gonzalez-Arroyo and M. Okawa, Phys. Rev. D **35**, 672 (1987).
- [7] E. Luijten and K. Binder, Phys. Rev. E **58**, R4060 (1998).
- [8] P. de Forcrand et al., Nucl. Phys. B **577**, 263 (2000).
- [9] C. Bagnuls and C. Bervillier, Phys. Rev. **B32**, 7209 (1985).
- [10] A. Pelissetto, P. Rossi, and E. Vicari, Phys. Rev. **E58**, 7146 (1998) and Nucl. Phys. **B554**, 552 (1999); A. Pelissetto and E. Vicari, cond-mat/0012164; S. Caracciolo *et al.*, cond-mat/0105160.
- [11] J. Gaite and D. O'Connor, Phys. Rev. D **54**, 5163 (1996).
- [12] M. Campostrini, J. Stat. Phys. **103**, 369 (2001).
- [13] Y. Meurice, G. Ordaz, and V. G. J. Rodgers, Phys. Rev. Lett. **75**, 4555 (1995).
- [14] Y. Meurice, S. Niermann, and G. Ordaz, J. Stat. Phys. **87**, 363 (1997).
- [15] K. Wilson, Phys. Rev. B. **4**, 3185 (1971).
- [16] F. Dyson, Comm. Math. Phys. **12**, 91 (1969).
- [17] G. Baker, Phys. Rev. B **5**, 2622 (1972).
- [18] Y. Meurice and S. Niermann, Phys. Rev. E **60**, 2612 (1999).
- [19] B. Nickel, in *Phase Transitions, Cargese 1980*, edited by M. Levy, J. L. Guillou, and J. Zinn-Justin (Plenum Press, New York, 1982).
- [20] P. Bleher and Y. Sinai, Comm. Math. Phys. **45**, 247 (1975).
- [21] P. Collet and J. P. Eckmann, *A Renormalization Group Analysis of the Hierarchical Model in Statistical Mechanics* (Springer-Verlag, Berlin, 1978).
- [22] H. Koch and P. Wittwer, in *Nonlinear Evolution and Chaotic Phenomena*, Nato ASI Series, Series B: Physics, Vol. 176, G. Gallavotti and P. Zweifel Editors, Plenum; and in *Mathematical Quantum Field Theory and Related Topics*, Canadian Mathematical Society, Conference Proceedings v. 9 (1988).
- [23] J. Godina, Y. Meurice, M. Oktay, and S. Niermann, Phys. Rev. D **57**, 6326 (1998).
- [24] J. Godina, Y. Meurice, and M. Oktay, Phys. Rev. D **57**, R6581 (1998) and **59**, 096002 (1999).
- [25] H. Koch and P. Wittwer, Math. Phys. Electr. Jour. **1**, Paper 6 (1995).
- [26] Y. Meurice, Phys. Rev. E **63**, 055101(R) (2001).
- [27] J. P. Eckmann and P. Wittwer, Jour. Stat. Phys. **46**, 455 (1987).
- [28] T. Niemeijer and J. van Leeuwen, in *Phase Transitions and Critical Phenomena*, vol. 6, edited by C. Domb and M. Green (Academic Press, New York, 1976).
- [29] L. Li and Y. Meurice, in preparation.
- [30] J. J. Godina, Y. Meurice, and M. Oktay, Phys. Rev. D **61**, 114509 (2000).

- [31] Y. Meurice and B. Oktay, Phys. Rev. D **63**, 016005 (2001).
- [32] A. Aharony and M. Fisher, Phys. Rev. B **27**, 4394 (1983).
- [33] A. Aharony and G. Ahlers, Phys. Rev. Lett. **44**, 782 (1980).
- [34] M. Chang and A. Houghton, Phys. Rev. Lett. **44**, 785 (1980).



## FIGURES

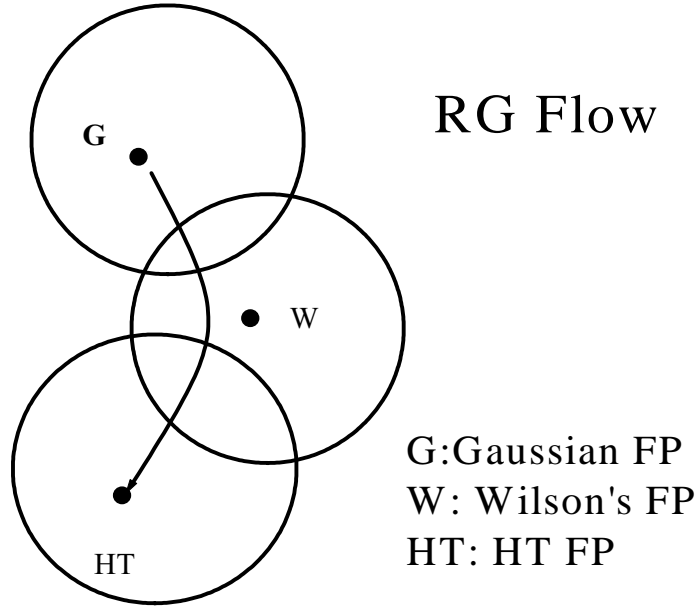


FIG. 1. Schematic representation of a RG flow starting near the Gaussian fixed point, passing near Wilson's fixed point and ending at the stable high-temperature fixed point. The circles represent the domains of validity of expansions of the scaling fields near the three fixed points.

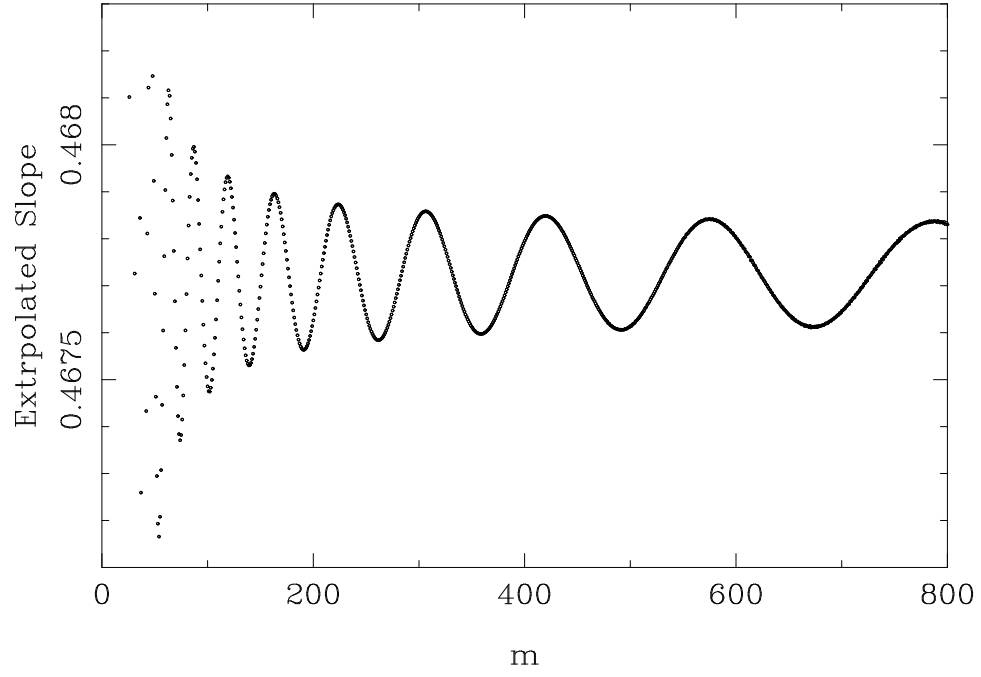


FIG. 2. The extrapolated slope ( $\hat{S}_m$ ) versus  $m$  for the HT of  $\chi$  calculated from the simplified recursion Eq. (4.2) with  $c = 2^{1/3}$ .

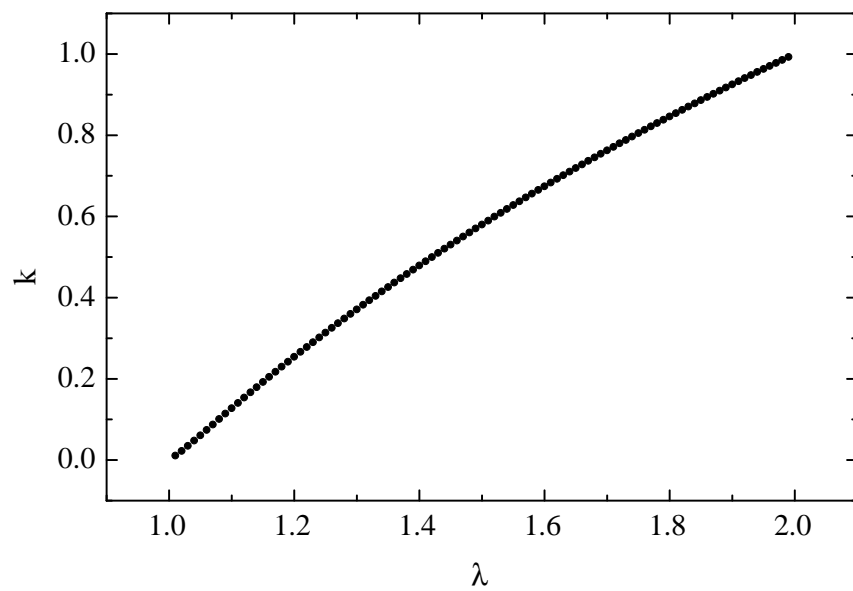


FIG. 3. The exponent  $k$  defined in Eq. (4.10) as a function of  $\lambda$ .

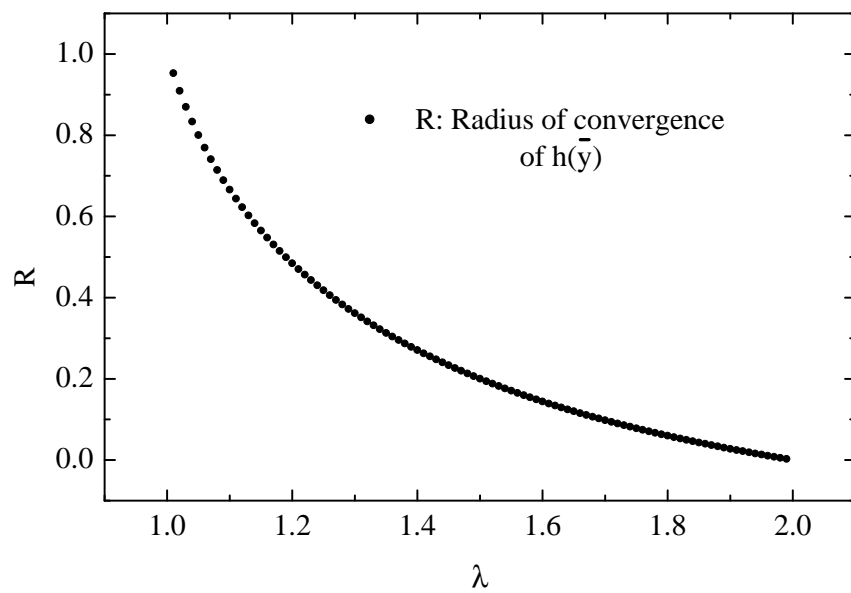


FIG. 4. Radius of convergence of  $h(\tilde{y})$  as a function of  $\lambda = 2 - \xi$ .

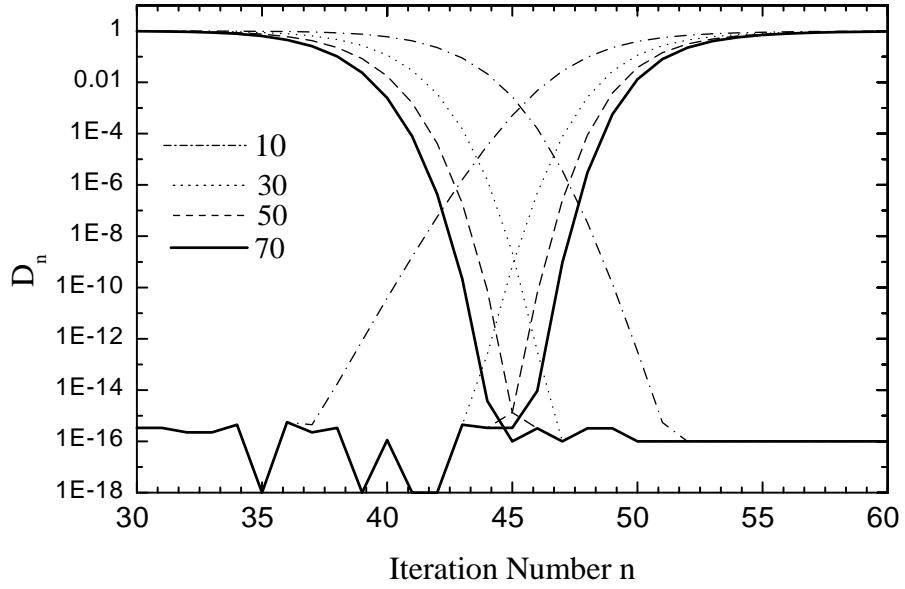


FIG. 5. Departure from scaling  $D_n$  defined in the text, for  $y$  (curves reaching 1 to the right) and  $\tilde{y}$  (curves reaching 1 to the left). In each cases, we have considered approximations of order 10 (dot-dashes), 30 (dots), 50 (dashes) and 70 (solid line). The value of  $\lambda$  is 1.5.

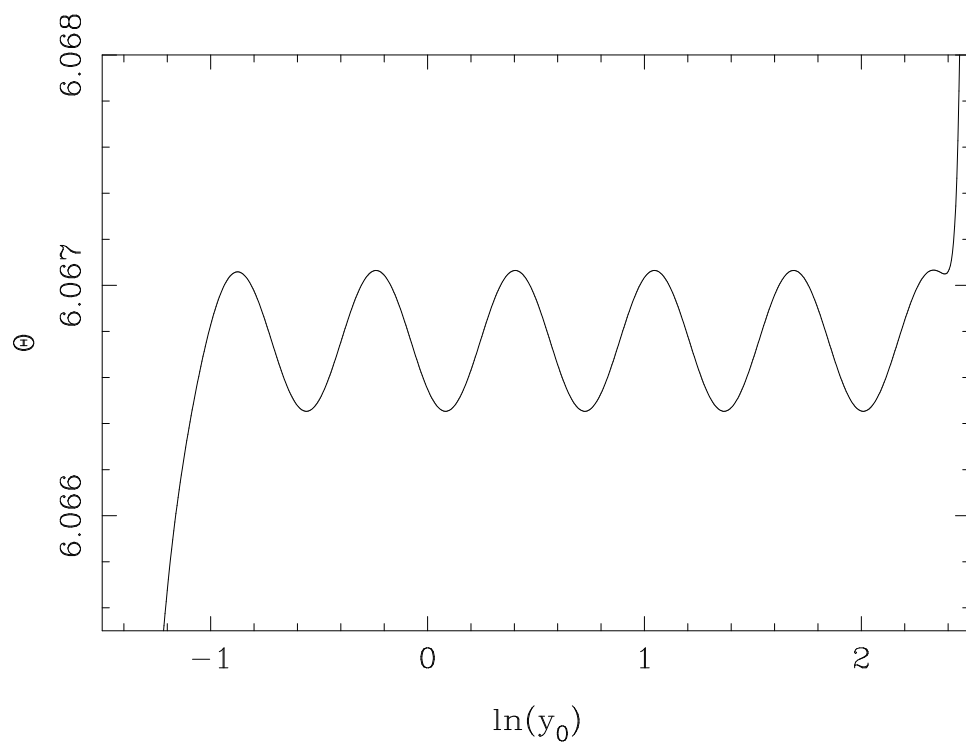


FIG. 6. The invariant function  $\Theta$ , calculated at  $\xi = 0.1$ , and plotted against  $\ln(y_0)$ .

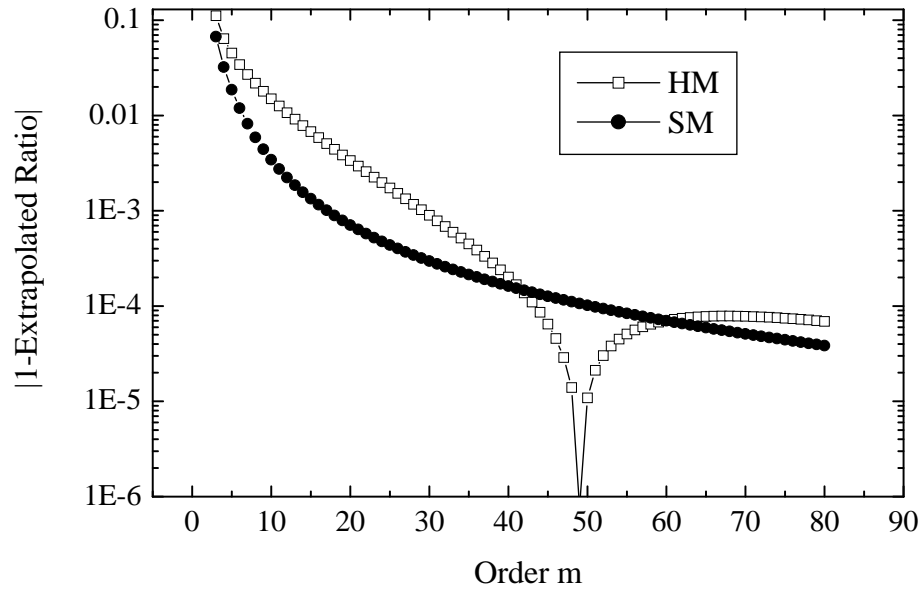


FIG. 7. The absolute value of the difference between the extrapolated ratio and 1 for the HM (empty boxes) and the SM (full circles), as a function of the order.

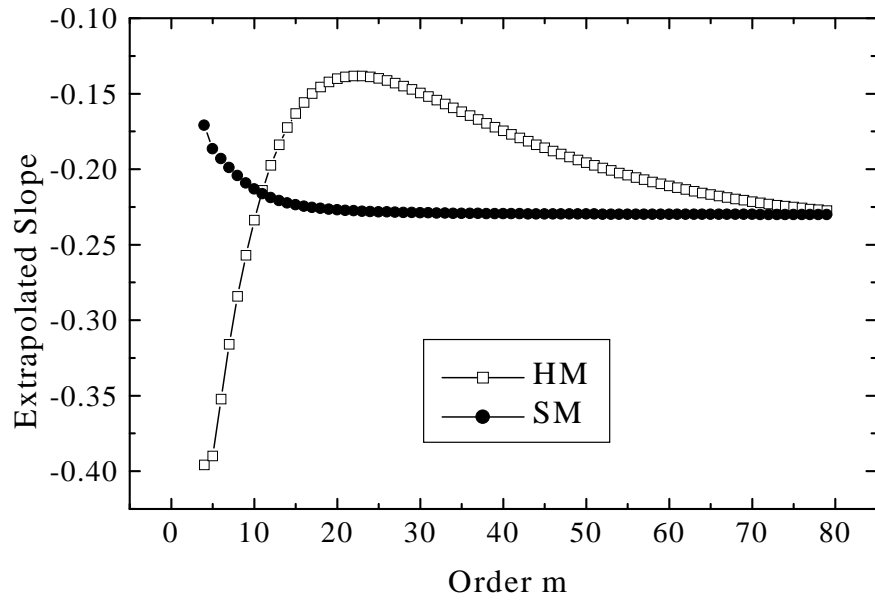


FIG. 8. The extrapolated slope  $\hat{S}_m$  for the HM (empty boxes) and the SM (full circles) as a function of the order .



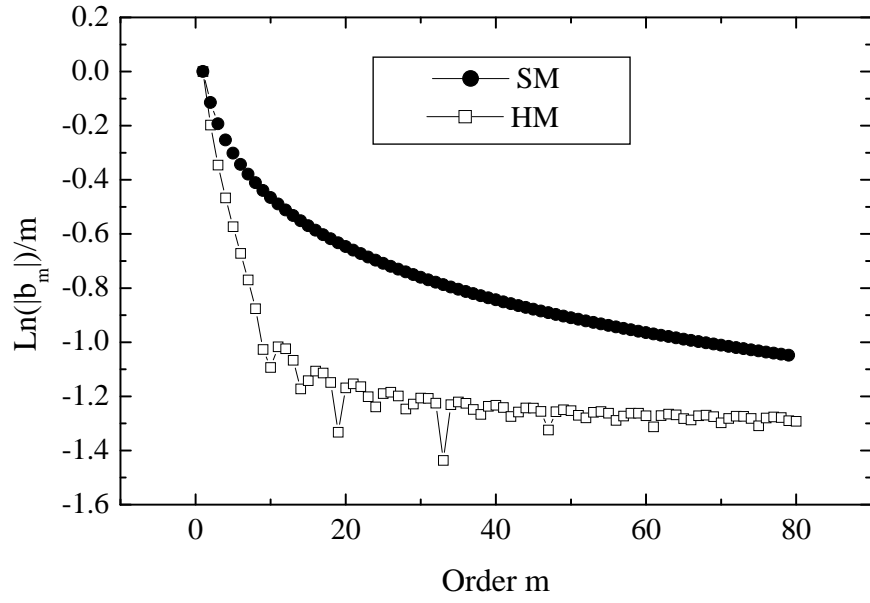


FIG. 9. Logarithm of the absolute value of the coefficients of the expansion of  $d_1(y_1)$  divided by the order, for the HM (empty boxes) and the SM (circles).

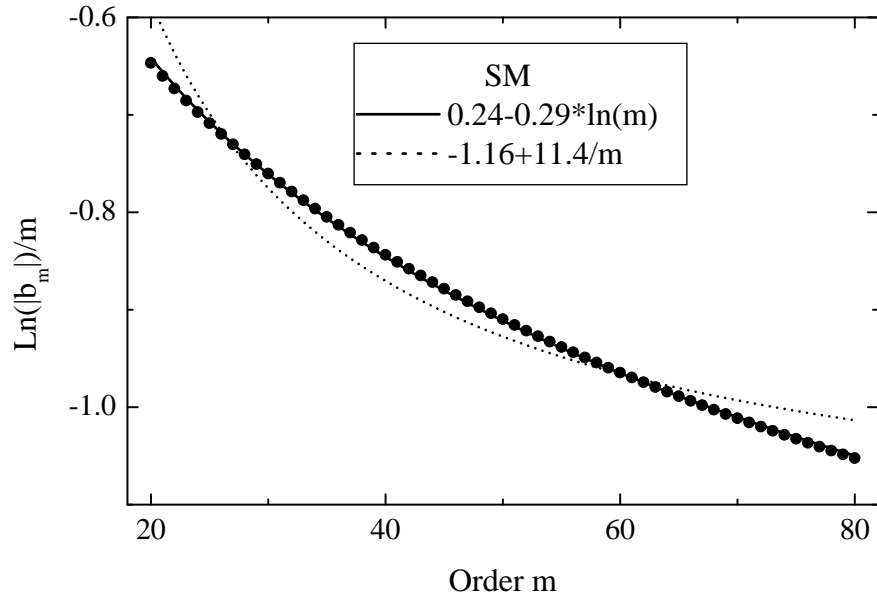


FIG. 10. Comparison of fits of the form  $A_1 + A_2/m$  (dots) and  $B_1 \ln(m) + B_2$  (solid line) with the data provided in Fig. 9 for the SM (circles).

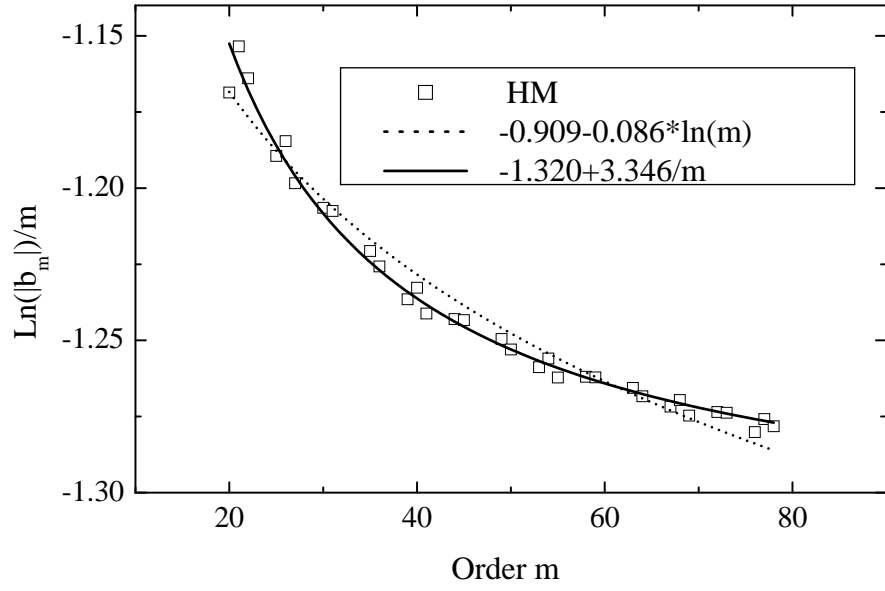


FIG. 11. Comparison of fits of the form  $A_1 + A_2/m$  (solid line) and  $B_1 \ln(m) + B_2$  (dots) with selected points of the data in Fig. 9 for the HM (boxes).

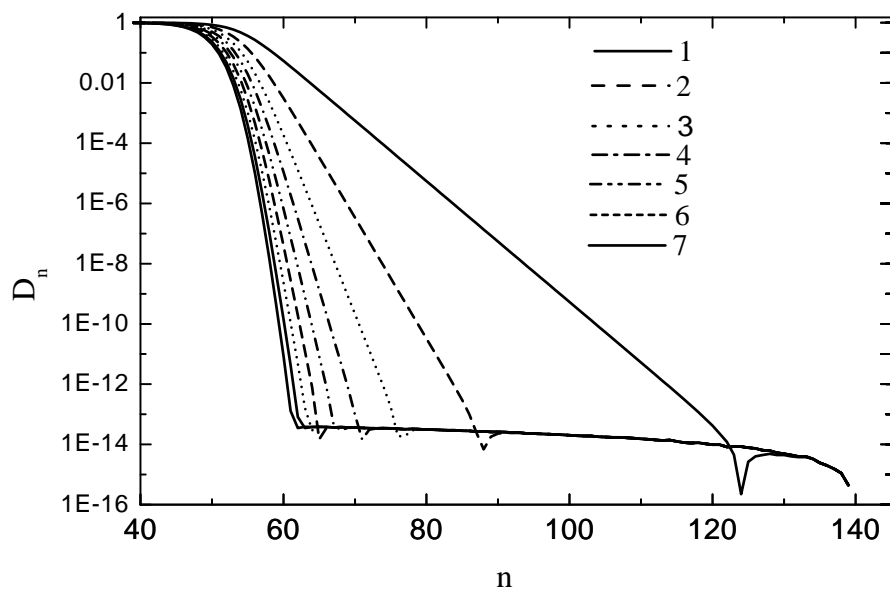


FIG. 12. The quantity  $D_n$  defined in Eq. (4.13) for expansions of  $\tilde{y}_1$  in  $\beta$ , at order 1 (solid line), 2 (dashes), 3 (dots), etc... for each iteration  $n$ .

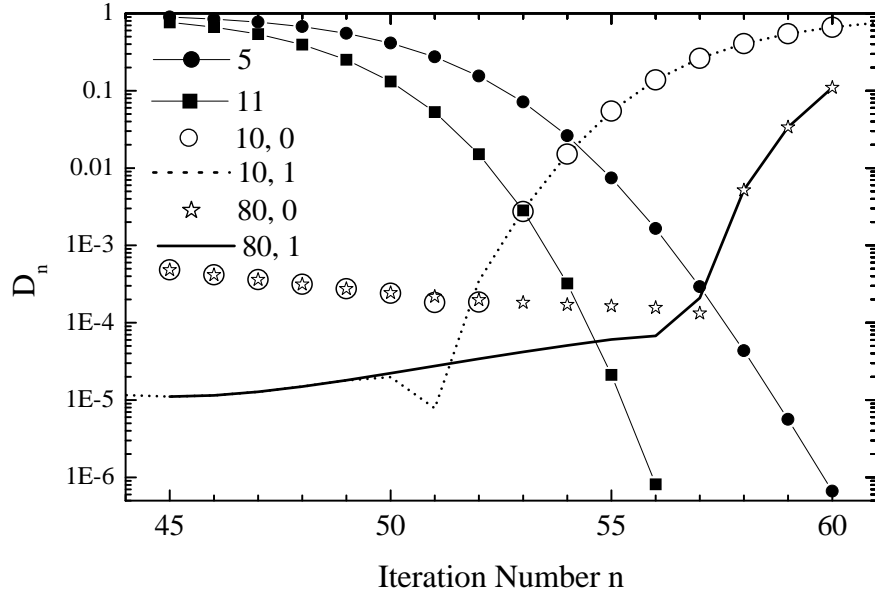


FIG. 13. Values of  $D_n$  for  $\tilde{y}_1$  up to order 5 in  $\beta$  (filled circle) and 11 (filled boxes), and for  $y_1$  up to order 10 in  $d_1$  (empty circles) and with first order corrections in  $y_2$  (dots), and up to order 80 in  $d_1$  (empty stars) and with first order corrections in  $y_2$  (solid line).

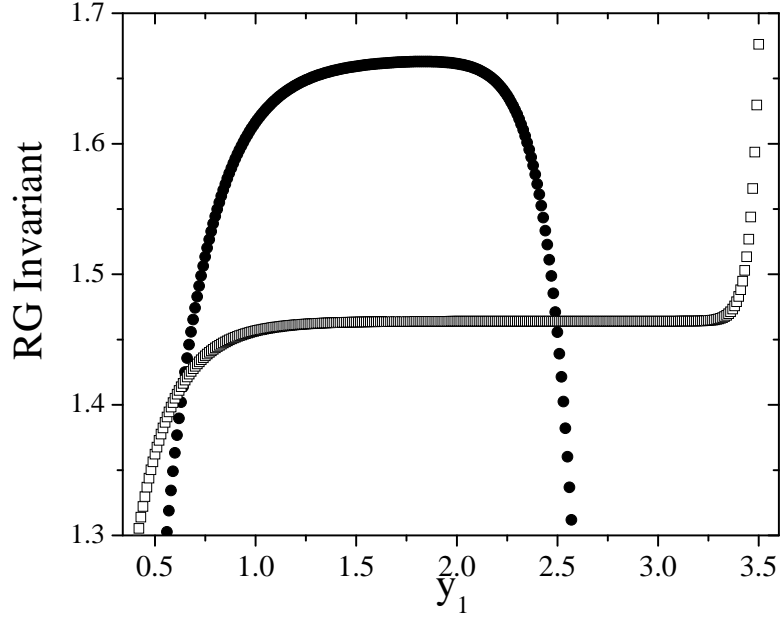


FIG. 14. Values of  $C_1$  (empty squares) and  $C_2$  (black circles) defined by Eq. (5.22), as a function of  $y_1$ .